DMD Fast Forward. Published on August 8, 2006 as doi:10.1124/dmd.105.006437

DMD #6437

Porcine Brain Microvessel Endothelial Cells (PBMEC) as an *In Vitro* Model to Predict *In Vivo* Blood-Brain Barrier (BBB) Permeability

Yan Zhang[1], Cheryl S. W. Li, Yuyang Ye, Kjell Johnson, Julie Poe,

Shannon Johnson, Walter Bobrowski, Rosario Garrido, and Cherukury Madhu[1]

Pharmacokinetics Dynamics and Metabolism (Y.Z., C.L., Y.Y., J.P., S. J., C.M.), Nonclinical Statistics (K.J.), Drug Safety Evaluation (W.B., R.G.), Pfizer Global Research and Development, 2800 Plymouth Road, Ann Arbor, MI 48105

a) Running Title: Prediction of brain penetration using blood-brain barrier cells

b) Corresponding author:

Dr. Cheryl S. W. Li

Department of Pharmacokinetics, Dynamics & Metabolism

Global Research & Development

Pfizer Inc.

2800 Plymouth Road

Ann Arbor, MI 48105

Phone: 734-622-1833

FAX: 734-622-3021

Email: cheryl.li@pfizer.com

c) Text Pages: 35

Figures: 8

Table: 4

References: 46

Number of Words in:

Abstract: 252

Introduction: 863

Discussion: 1590

d) Abbreviations

ACM, astrocyte-conditioned medium; BBB, blood-brain barrier; BBMEC, bovine brain microvessel endothelial cells; BCRP, breast cancer resistant protein; CNS, central nervous system; GAPDH, glyceraldehyde-3-phosphate dehydrogenase; GLUT, glucose transporter; OATP, organic anion transporting polypeptide; PBMEC, porcine brain microvessel endothelial cells; LAT, system L amino acid transporter; MRP, multidrug resistance-associated protein; NCEs, new chemical entities; P_{app}, apparent *in vitro* permeability coefficient; P_e, effective *in vitro* permeability coefficient; PS, permeability surface product; Pgp, P-glycoprotein; RT-PCR, reverse transcription-polymerase chain reaction; TEER, transendothelial electrical resistance; UWL, unstirred water layer.

Abstract

The objective of the study was to establish primary cultured porcine brain microvessel endothelial cells (PBMEC) as an *in vitro* model to predict the blood-brain barrier (BBB) permeability *in vivo*. The intercellular tight junction formation of PBMEC was examined by electron microscopy and measured by Transendothelial Electrical Resistance (TEER). The mRNA expression of several BBB transporters in PBMEC was determined by RT-PCR analysis. The *in vitro* permeability of 16 structurally diverse compounds, representing a range of passive diffusion and transporter-mediated mechanisms of brain penetration, was determined in PBMEC. Except for the perfusion flow rate marker diazepam, the BBB permeability of these compounds was determined either in our laboratory or reported in literature using *in situ* brain perfusion technique in rats. Results in the present study showed that PBMEC had a high endothelium homogeneity, an mRNA expression of several BBB transporters, and high TEER values. Culturing with rat astrocyte-conditioned medium increased the TEER of PBMEC, but had no effect on the permeability of sucrose, a paracellular diffusion marker. The PBMEC permeability of lipophilic compounds measured under stirred conditions was greatly increased compared to measured under unstirred conditions. The PBMEC permeability of the 15 test compounds, determined under the optimized study conditions, correlated with the *in situ* BBB permeability with an r^2 of 0.60. Removal of the three system L substrates increased the r^2 to 0.89. In conclusion, the present PBMEC model may be used to predict or rank the *in vivo* BBB permeability of new chemical entities (NCEs) in a drug discovery setting.

Introduction

One major hurdle of successful central nervous system (CNS) drug delivery is to penetrate the blood-brain barrier (BBB) to reach the therapeutic targets. The BBB is a continuous layer of endothelial cells that are connected to each other through tight junctions. In contrast to the endothelial cells of peripheral blood vessels, the brain microvessel endothelial cells are characterized by unique intercellular tight junctions, the absence of fenestrations, and minimal pinocytic activity. The BBB represents a physiological barrier that efficiently restricts free paracellular passage of most substances from the blood to the brain extracellular environment. Furthermore, the brain microvessel endothelial cells possess a variety of metabolic enzyme systems, which further limit the brain entry of compounds (Pardridge 1983). Finally, a complex of membrane-bound transport systems, including active efflux transporters, such as P-glycoprotein (Pgp) (Schinkel et al. 1996; Miller et al. 2000) and Multidrug Resistance-Associated Protein (MRP) (Miller et al. 2000; Zhang et al. 2000), and active uptake transporters such as the system L amino acid transporter (LAT) (Pardridge 1983; Smith 1991), further regulates brain penetration.

Pharmaceutical companies have been actively pursuing various methods to accurately predict the brain penetration of new chemical entities (NCEs) at an early stage of drug discovery. Currently, several approaches are available for assessing brain penetration of NCEs, but they often pose a compromise between high throughput with low predictive potential and low throughput with high predictive potential. Passive diffusion permeability of NCEs may be predicted by high-throughput *in silico* modeling approaches based on the physical-chemical parameters (Liu et al. 2004). However, current *in silico* models do not account for metabolism, transporter-mediated processes, or any other drug-membrane or drug-protein interactions that

may affect the ability of a drug to cross the BBB. With *in vivo* approaches (i.e. equilibrium brain-to-plasma distribution ratios (logBB) and BBB permeability-surface area product (logPS)) (Oldendorf 1971; Smith 1996), high-throughput models that can accommodate screening of a large number of compounds in early discovery are difficult to develop. Thus, a well-characterized *in vitro* BBB cell model, which has the potential to account for the complex molecular interactions underlying BBB permeability and function as a moderate throughput screening tool for NCEs would be highly useful in the discovery process.

A range of *in vitro* BBB cell models, including primary cultured/low passage brain microvessel endothelial cells and immortalized brain microvessel endothelial cell lines have been generated by various academic laboratories. However, none of these models have been established as a widely used BBB permeability screen within the pharmaceutical industry. In recent years, the time and resource-sparing advantages have made immortalized BBB cell models such as conditionally immortalized rat brain microvessel endothelial cells (TR-BBB) (Terasaki and Hosoya 2001) attractive options. However, characterizations of immortalized BBB cell lines (Terasaki and Hosoya 2001; Reichel et al. 2002) and initial investigations in our laboratory with TR-BBB cells (data not shown) suggest that immortalized cell cultures generally fail to form a sufficiently tight barrier for use in permeability studies. Primary cultured bovine brain microvessel endothelial cells (BBMEC), first developed by Bowman et al. (1983) and subsequently modified in Borchardt's laboratory (Audus and Borchardt 1986a; Audus and Borchardt 1986b; Miller et al. 1992), have been the most extensively investigated *in vitro* BBB model. Primary cultures of BBMEC phenotypically maintain many *in vivo* BBB characteristics such as tight junction formation and expression of active transporter proteins and metabolic enzymes. However, despite observation of a strong qualitative correlation between *in vitro*

BBMEC transcellular permeability and logBB (Guillot et al. 1993; Saheki et al. 1994; Cecchelli et al. 1999), a solid quantitative correlation derived from a structurally diverse set of compounds, representing passive and active brain penetration, is still lacking. Beginning in 1998, several groups have assessed the use of primary porcine brain microvessel endothelial cells (PBMEC) for *in vitro* permeability studies (Franke et al. 2000; Jeliazkova-Mecheva and Bobilya 2003; Torok et al. 2003). It has been suggested that the PBMEC model may offer a more restrictive paracellular pathway as compared with the BBMEC model (Franke et al. 2000). However, literature data regarding the tightness of cellular junctions of BBMEC or PBMEC models have been highly variable due to differences in cell isolation procedures, cell culture and experimental conditions among laboratories (Fischer et al. 2000; Jeliazkova-Mecheva and Bobilya 2003; Torok et al. 2003).

The purposes of the current study were to develop a primary cultured PBMEC model under optimized study conditions and to evaluate its use as a moderate to high throughput screening tool to predict *in vivo* BBB transport of structurally diverse compounds with passive and/or active brain penetration. To achieve this goal, we first developed a PBMEC culture and evaluated how well the PBMEC retain the characteristics of *in vivo* BBB in terms of endothelial origin, expression of BBB transporters, and tight-junction formation. Following the initial characterization, we evaluated a number of culture and experimental variables to optimize study conditions. Lastly, the ability of the PBMEC model to predict *in vivo* BBB penetration was evaluated by comparing the trans-endothelial permeability measured in the PBMEC model with the BBB penetration determined by *in situ* brain perfusion for a set of 16 structurally diverse compounds, representing a range of passive diffusion and transporter-mediated mechanisms of brain penetration.

Materials and Methods

Materials and reagents

[^{14}C]-sucrose (600 mCi/mmol), [^{14}C]- diazepam (55 mCi/mmol), and [^{3}H]-dopamine (9 Ci/mmol) were obtained from Amersham Biosciences (Buckinghamshire, UK). [^{3}H]-methotraxate (16.9 Ci/mmol), [^{14}C]- phenytoin (53.1 mCi/mmol), [^{14}C]- caffeine (53 mCi/mmol), [^{3}H]- vinblastine (5.9 Ci/mmol), [^{3}H]- metoprolol (60.4 Ci/mmol), and [^{3}H]-theophylline (13.3 Ci/mmol) were purchased from Moravek Biochemicals (Brea, CA). [^{3}H]-Mannitol (17 mCi/mmol) and [^{3}H]-taurocholic acid (2 Ci/mmol) were purchased from PerkinElmer Life and Analytical Sciences (Boston, MA). [^{3}H]- quinidine (20 Ci/mmol), [^{3}H]-testosterone (90 Ci/mmol), [^{3}H]- leucine (60 Ci/mmol), and [^{3}H]- phenylalanine (80 Ci/mmol) were obtained from American Radiolabeled Chemicals Inc. (St. Louis, MO). [^{3}H]-gabapentin (44.15 Ci/mmol) was synthesized in-house.

Minimum Essential Medium (MEM), Ham's F-12 medium, Dulbecco's modified Eagle's Medium (DMEM) with low glucose, and rat tail collagen were purchased from Fisher Scientific (St. Louis, MO). Fibronectin and equine serum were purchased from Sigma Chemical Company (St. Louis, MO). Dispase and collagenase/dispase were obtained from Roche Diagnostics (Indianapolis, IN). Tissue culture Transwell^{TM} inserts (24 mm diameter, 0.4 μm pore size, Costar Corp.) were obtained from VWR (Chicago, IL). Side-by-side horizontal diffusion chambers, chamber clamps, and H1 stirrer were purchased from PermeGear, Inc. (Bethlehem, PA).

Selection of compounds for method development

Sixteen structurally diverse compounds were selected for the evaluation of the present PBMEC model. As shown in Table 1, the compounds chosen are of diverse chemical classes, represent both passive diffusion and carrier-mediated BBB uptake or efflux processes (Hargreaves and Pardridge 1988; Drion et al. 1996; Kitazawa et al. 1998; Kusuhara et al., 1997; Martel et al., 1996; McCall et al., 1982; Miller et al. 2000; Potschka and Loscher 2001; Su et al., 1995). In addition, the BBB permeability of these compounds determined by *in situ* brain perfusion ranged from low to high (Murakami et al. 2000; Liu et al. 2004). The logPS of 8 test compounds (taurocholic acid, methotrexate, theophylline, phenytoin, caffeine, dopamine, phenylalanine, and testosterone) were reported by Liu et al. (Liu et al. 2004). The logPS of sucrose, mannitol, vinblastine, and quinidine were reported by Murakami et al. (Murakami et al. 2000), and the logPS of gabapentin, leucine, and metoprolol were determined in our laboratory. The highly permeable compound diazepam was used as the regional flow rate marker in brain perfusion studies (Liu et al. 2004); therefore, logPS value of diazepam was not calculable.

Isolation of Porcine Brain Microvessel Enodothelial Cells (PBMEC)

PBMEC were isolated from fresh porcine brains using a combination of enzyme digestion and ultra-centrifugation approaches as previously described (Miller et al. 1992) with minor modifications. Briefly, fresh porcine brains were obtained from a local slaughterhouse. The surface vessels and meninges of the brains were removed under aseptic conditions. The gray matter was collected by aspiration and then homogenized by sequential passing of the brain materials through a 1000 μm, then a 710 μm screen. The filtrate was digested with 12.5% (wt/vol) dispase for three hours followed by centrifugation at 1570×g for ten minutes. The pellet

was resuspended in 13% (wt/vol) dextran followed by a centrifugation at 9170×g for ten minutes. After centrifugation, the supernatant was discarded and the dark red pellet was collected and subjected to further enzyme digestion in 0.52% (wt/vol) collagenase/dispase for 3.5 hours. Following the incubation, the endothelial cells were separated from cellular debris and red blood cells by Percoll gradient centrifugation at 1700×g for ten minutes. The average yield of PBMEC was approximately 10 x 10^6 cells/ brain. For cell preservation, cells were frozen in MEM:F12 media supplemented with 10% DMSO, 20% horse serum, 50 μg/ml gentamicin, 2.5 μg/ml amphotericin B, and 100 μg/ml heparin and stored in liquid nitrogen.

Isolation of rat astrocytes

Rat astrocytes were isolated from the cerebral cortex of newborn pups (1-2 day old) according to the method of McCarthy and de Vellis (McCarthy and de Vellis 1980). Briefly, the cortices, free of meninges, were dissected in Hanks' balanced salt solution (Ca^{2+} and Mg^{2+}-free) and incubated in 0.125% trypsin at 37°C for ten min followed by three washes with DMEM medium supplemented with 10% FBS, 1 U/ml penicillin and 1 mg/ml streptomycin. After the washing, cells were resuspended in the same medium and filtered through a nylon mesh with a pore size of 100 μm. Filtered cells were seeded on poly-D-lysine-coated culture flasks at a density of 1.5 x 10^5 cells/cm^2. On culture day nine, the oligodendrocytes and microglia were removed from the astrocyte cultures by vigorous shaking at a speed of 250 rpm at 37°C overnight. Astrocytes were seeded at a density of 2.4 x 10^5 cells/cm^2 in poly-D-lysine coated culture flasks for collection of astrocyte-conditioned medium (ACM). ACM was collected after 48 hr incubation, and was sterile-filtered. The ACM was used either immediately or stored at –20°C for future use.

Culture of cells

The freshly isolated or cryopreserved PBMEC cells were seeded (7.5×10^4 cells/cm^2) on collagen-coated, fibronectin-treated polycarbonate Transwell™ membranes and cultured in MEM:F12 media supplemented with 10% horse serum, 50 μg/ml gentamicin, 2.5 μg/ml amphotericin B, and 100 μg/ml heparin. For PBMEC culture in the absence of ACM, the MEM:F12 growth media was added to the top and bottom wells, and was renewed every other day until the cells reached confluence (typically five to six days). For PBMEC culture with ACM, the MEM:F12 growth medium from the bottom well of the Transwell plates was replaced by the ACM once the PBMEC reach near-confluence around day 4 in culture. Fresh MEM:F12 growth medium for PBMEC was added to the top well of the Transwell plates. The PBMEC cells were then incubated for another two to four days in the humidified 37°C incubator with 5% CO_2 supply before beginning the permeability studies.

Electron Microscopy for PBMEC

PBMEC monolayers grown in collagen-coated, fibronectin-treated Transwell™ inserts were fixed with 2% (wt/vol) paraformaldehyde and 2.5% (vol/vol) glutaraldehyde in 0.1 M sodium cacodylate (pH 7.4) containing 5% (wt/vol) sucrose. The cell monolayers were then post-fixed in 0.1M sodium cacodylate buffer containing 1% (wt/vol) osmium tetroxide, 0.5% (wt/vol) potassium ferricyanide, and 5% (wt/vol) sucrose for 1 h and embedded. The cells were visualized through an FEI-Philips CM100 BioTwin electron microscope operated at 60 kV. Imaging was performed with a Kodak 4.2i digital camera from Advanced Microscopy Techniques, Inc. (Danvers, MA).

Histocytochemistry for PBMEC

PBMEC grown on LabTek glass chambered slides (Nalge Nunc International Corp., Naperville, IL) were fixed in ice-cold 80% methanol for 20 minutes, and air-dried for 1 hour. Non-specific staining was blocked by incubation with serum-free protein blocker (DakoCytomation, Carpinteria, CA) for 30 minutes. The cells were first incubated with primary antibodies (1:100 dilution) of either rabbit polyclonal anti-von Willebrand Factor (Factor VIII) (DakoCytomation, Carpinteria, CA) or normal rabbit IgG as negative controls for one hour at room temperature. Cells were then incubated with a secondary anti-rabbit biotinylated antibody (Vector Laboratories, Burlingame, CA) for another 45 minutes, followed by application of streptavidin-Alexa Fluor 488 (Molecular Probes, Eugene, OR) for 35 minutes. Cells were counterstained with the nuclear dye DAPI (Molecular Probes, Eugene, OR) for ten minutes, and then mounted with ProLong mounting media (Molecular Probes, Eugene, OR). Cell staining was visualized using a Zeiss Axiovert 200 fluorescent microscope equipped with fluorescent filters for FITC and DAPI visualization. Images for the two fluorescent channels were collected separately and combined using the Axiovision software package (Zeiss, Thornwood, NY).

Reverse Transcription-Polymerase Chain Reaction (RT-PCR) in PBMEC

The mRNA expression of various transporters was determined by RT-PCR using glyceraldehyde-3-phosphate dehydrogenase (GAPDH) as an internal control. The primers used for each gene are listed in Table 2. Total RNA from confluent PBMEC monolayers was isolated using an RNeasy Mini Kit (QIAGEN, Valencia, CA) according to manufacturer's instructions. RT-PCR was accomplished by using "SuperScript^{TM} One-Step RT-PCR with Platinum^{R} Taq"

(Invitrogen, Carlsbad, California). The reaction of RT was carried out at 50°C for 30 min. For all transporters and the reference gene GAPDH, identical thermal cycling conditions for PCR were used: 2 minutes at 94^{o}C to denature followed by 35 cycles of 94^{o}C for 15 seconds, 55^{o}C for 30 seconds, and 68^{o}C for 45 seconds. The products (20 μl) from the PCR amplification were separated on 2% agarose gel and stained with ethidium bromide to check product integrity. The identity of the selected positive RT-PCR products was verified with sequence analysis.

Transendothelial Electrical Resistance (TEER) Measurement with PBMEC

The TEER was used as a measure of tight junction formation by the PBMEC monolayers. The TEER value (Ω) was determined using an EndOhm Chamber connected to an EVOM resistance meter (World Precision Instruments, Inc. Sarasota, FL), and reported as Ω•cm^2 after correcting for the surface area of the membrane (4.5 cm^2). The EndOhm system provided a more reproducible TEER measurement as compared with the traditional "chopstick" electrode system. The variation of resistance measured from the same membrane insert was approximately 3 and 30 Ω•cm^2 using the EndOhm and "chopstick" systems, respectively (data not shown). The TEER value of a blank membrane was subtracted from the apparent TEER values of membranes with cells to obtain the effective TEER value of the PBMEC monolayer. In order to use cells with ideal tight junction formation, TEER values were monitored from day 4 to day 13 for various PBMEC cultures. No permeability studies were performed when the TEER values were below 300 Ω•cm^2.

In vitro Permeability Studies in PBMEC

The *in vitro* permeability studies in PBMEC were performed as described by Mark and Miller (Mark and Miller 1999) with minor modifications. Confluent PBMEC cells were pre-incubated with assay buffer (122 mM NaCl, 25 mM Na_2CO_3, 10 mM D-glucose, 3 mM KCl, 1.2 mM $MgSO_4 \cdot 7H_2O$, 0.4 mM K_2HPO_4, 1.4 mM $CaCl_2$, 10 mM HEPES, pH 7.4) for 30 min at 37^{o}C. After pre-incubation, the filter membranes, with or without a PBMEC monolayer, were cut off from the Transwell inserts and placed between donor and receiver chambers in a side-by-side diffusion chamber. At time 0, 3 ml of assay buffer containing ^{14}C-radiolabeled sucrose (1 μCi/ml) as a paracellular diffusion marker and ^{3}H-radiolabled test compounds (0.2 μCi/ml) were added into the donor chamber facing the apical side of the cell monolayer. When using ^{14}C-caffeine, ^{14}C-phenytoin, or ^{14}C-diazepam as test compounds, ^{3}H-mannitol was used as the paracellular diffusion marker instead. The temperature of the medium in the donor and receiver chambers was maintained at 37^{o}C by a continuous flow of water generated from a temperature-regulating circulating bath (Lauda E100, Brinkmann Instruments Inc., Westbury, NY). At 0, 5, 10, 20, and 40 minutes after adding test compound, 10 μl and 3 ml samples were taken from donor and receiver chambers, respectively. For the substrates of efflux transporters, including vinblastine, quinidine, and methotrexate, the last sample was taken at 60 min. The receiver chamber was immediately replaced with 3 ml of blank assay buffer after removal of each sample. The experiment was performed at 37^{o}C under either unstirred or well-stirred (600 rpm) conditions. Radioactivity levels of the samples collected from the donor (10 μl) and receiver (50 μl) chambers were determined using a liquid scintillation counter (Packard, Tri-Carb).

The apparent *in vitro* permeability coefficient of a compound (P_{app}) was obtained from the slope of the linear plot of compound flux into the receiver chamber over time according to the following equation:

$$P_{app} = Flux / (C_{D,t}*A) = (M_{R,t}/t) / (C_{D,t}*A)$$

where $C_{D,t}$ is the concentration of the compound in the donor chamber at time t; $M_{R,t}$ is the amount of compound in the receiver chamber at time t; and A is the surface area of the membrane exposed between the side-by-side chamber (0.636 cm^2).

The effective permeability of a compound (P_e) was determined according to the following equation:

$$1/P_e = 1/P_{app} - 1/P_m$$

where P_m is the permeability of the compound across a collagen-coated, fibronectin-treated membrane without cells.

Because both P_{app} and P_m followed a normal distribution for the tested compounds, the standard error (SE) of the P_e was approximated using the Delta method as follows (Casella and Berger 1990):

$$SE_e^2 = \frac{1}{d}\sum_{i=1}^{d}\left[\left(\frac{\overline{P}_{m,i}^2}{\left(\overline{P}_{m,i} - \overline{P}_{app,i}\right)^2}\right)^2 SE_{P_{app,i}}^2 + \left(\frac{\overline{P}_{app,i}^2}{\left(\overline{P}_{m,i} - \overline{P}_{app,i}\right)^2}\right)^2 SE_{P_{m,i}}^2\right]$$

where *d* equals the number of days on which experiments were conducted to determine P_{app} and P_m.

<u>*In Situ* Rat Brain Perfusion and Data Analysis</u>

The *in vivo* blood-to-brain influx permeability for gabapentin, leucine, and metoprolol was determined in our laboratory using the *in situ* rat brain perfusion technique reported by

Smith et al. (Smith 1996). Briefly, male Sprague-Dawley rats (300-350 g, Charles River Breeding Laboratories, Portage, MI) were anesthetized intramuscularly with ketamine (80mg/ml) and xylazine (12mg/ml) at a dose of 0.1 ml/100g BW. After exposure of the right carotid artery, the external carotid artery and pterygopalatine artery were ligated. The right common carotid artery was cannulated with a PE50 tubing filled with sodium heparin saline (100 IU/ml). After the cannula was in place, the ventricle of the heart was severed and the rats were perfused with Krebs Ringer perfusion fluid (2.4 mM NaH_2PO_4, 4.2 mM KCl, 24 mM $NaHCO_3$, 128 mM NaCl, 1.5 mM $CaCl_2$, 0.9 mM $MgSO_4$) for 10 to 40 seconds at a rate of 10 ml/min using a perfusion pump. ^{3}H-labeled gabapentin, leucine, or metoprolol was added to the oxygenated and bicarbonate-buffered perfusate to yield a final perfusion concentration of 0.3-0.5 µCi/ml for each compound. The perfusion was terminated by stopping the pump. The rats were decapitated, and brains were immediately excised. The excised brains were stored at -20°C until analysis. For the analysis of radioactivity in the brain cortex, the tissues were homogenized in 3 volumes (w/v) of water. An aliquot of brain homogenate (0.1 ml) were digested at 50°C overnight in 1 ml of tissue solubilizer. After cooling, the samples were prepared for scintillation counting by addition of 15 ml of scintillation cocktail. To determine the concentration of compound in the perfusion fluid, an aliquot of 20 µl of perfusion fluid was placed in a scintillation vial containing 15 ml of scintillation cocktail. The radioactivity in the brain or perfusion fluid samples was measured with a liquid scintillation counter (Packard, Tri-Carb).

The brain uptake constant (K_{in}) was calculated from the following equation:

$$A_{br}/C_{pf}=K_{in}*T+V_v$$

where A_{br} is the brain tissue concentration (dpm/g); C_{pf} is the perfusion fluid concentration (dpm/ml); T is the perfusion time (s); and V_v is the brain vascular volume (ml/g). K_{in} was estimated from the slope of the initial linear portion of A_{br}/C_{pf} versus T plot.

The permeability surface product (PS) (μl/s/g) was calculated from the following equation: $PS = -F \times \ln(1-K_{in}/F)$

where F is the regional flow rate estimated from diazepam K_{in} data (70 μl/s/g) (Liu et al. 2004).

Results

Morphology of the PBMEC Monolayer

Porcine brain microvessel endothelial cells grown on collagen-coated, fibronectin-treated culture dishes retained the characteristic morphology of capillary endothelial cells (Fig. 1a-1c). On day 2 in culture, the cells preferentially grew in clusters (Fig. 1a). They showed cobblestone-shaped morphology on day 4 in culture (Fig 1b). When the cells reached confluence on day 6 (Fig. 1c), PBMEC formed a continuous monolayer with an elongated, spindle-shaped morphology, which is typical for differentiated capillary endothelial cells. After another 3-4 days in culture, post-confluent cells developed multiple layers with some contaminated astrocytes and fibroblasts (data not shown).

Immunocytochemical Characterization of PBMEC

The PBMEC demonstrated extensive positive immunostaining for Factor VIII, an endothelial cell marker, predominantly in the cytoplasm with a characteristic granular and diffused staining pattern (Fig. 2a). There was no fluorescent staining in the negative control

where primary anti-rabbit IgG was applied instead of anti-Factor VIII antibody (Fig. 2b). Electron microscopic examination of confluent PBMEC showed the cells grew into a confluent monolayer on top of the collagen/fibronectin coated Transwell inserts with apparent intercellular tight junction formation (Fig. 3a-3d, indicated by arrows). The cells were linked to each other either by an overlapping membrane (Fig. 3a-3b) or direct contact (Fig. 3c-3d). Regardless of the type of connection, the tight junctions were consistently localized towards the apical side of the cell membranes (Fig. 3a-3d, indicated by arrows). Furthermore, the *in vitro* cultured PBMEC resembled *in vivo* BMECs in that there were no fenestrations, few pinocytotic vesicles, and an abundance of mitochondria.

Transporter Expression in PBMEC

As shown in Figure 4, positive RT-PCR products of corresponding size were detected in the PBMEC for a tight junction-associated protein, specifically ZO-1, several BBB uptake transporters, including the glucose transporter 1 (GLUT1), system L amino acids transporters 1 and 2 (LAT1 and LAT2), and efflux transporters including P-gp, MRP1, MRP4, MRP5, and breast cancer resistant protein (BCRP). MRP2 was not detected in current study. The sequence for the RT-PCR product of BCRP, of which the primers were designed based on porcine sequence, showed 99% homology to their porcine gene. The sequence for the RT-PCR product of MRP4, of which the primers were designed based on human and rodent MRP4 conservative regions, showed 89% and 84% identity to their corresponding human and rodent genes, respectively.

TEER of PBMEC monolayer

Prior to each transendothelial permeability study, the "tightness" of the PBMEC monolayer was assessed by TEER measurement. Figure 5 demonstrates the change of TEER values with duration of culture. The TEER values were slightly varied from one primary culture to another. The TEER values typically ranged from 300 to 550 $\Omega \bullet cm^2$ on day 5 to day 9 post-seeding. After 9 days in culture, the TEER values started to decline.

TEER values obtained from PBMEC cultured with ACM of one representative study are shown in Figure 6. The results showed that culture with ACM significantly enhanced the TEER values of PBMEC by 10 – 25% on culture days 6 through 9, post-seeding.

Permeability Measurement in PBMEC

Sucrose permeability, a measure of paracellular flux, was compared between PBMEC cultured in the presence and absence of ACM. Although culture with ACM enhanced the TEER values of PBMEC (Fig. 6), it had no effect on the P_e of the paracellular marker, sucrose (data not shown).

To test the influence of stirred versus unstirred conditions on compound permeability in the PBMEC cultures, the permeability of eight test compounds, including sucrose as a paracellular marker, was examined under both conditions. As shown in Table 3, stirring in both donor and receiver chambers (600 rpm) increased the *in vitro* permeability of the medium and high permeability compounds (i.e., caffeine, metoprolol, testosterone, and diazepam) but had little effect on the low permeability compounds (sucrose, mannitol, taurocholic acid, and vinblastine). The dynamic range (i.e. ratio of diazepam P_e to sucrose P_e) in this PBMEC model was enhanced from 34.8 under unstirred conditions to 62.8 under stirred conditions.

To assess the possibility of using cryopreserved PBMEC cultures for determination of the *in vitro* permeability of compounds, the average $logP_e$ values for 16 compounds determined in fresh and frozen cells under stirred conditions were statistically compared for similarity. As shown in Figure 7, the average $logP_e$ had strong agreement between fresh and cryopreserved cell preparations. Using the Total Deviation Index (TDI) (Lin, 2000), the average $logP_e$ values for 95% of the measured compounds from fresh and frozen cell preparations fall within 0.16 log units of each other.

In the subsequent permeability studies, the $logP_e$ of the 16 compounds was determined in PBMEC solo-culture under stirred conditions using both fresh and cyropreserved cells.

In vitro-to-*in situ* correlation

Table 4 summarizes the *in vitro* permeability of the 16 selected compounds as determined by the PBMEC model. The PBMEC cultures demonstrated a large dynamic range, with P_e values ranging from 92 to 3702 $x10^{-6}$ cm/second for the 16 compounds. In addition, the rank order of the PBMEC permeability was comparable with that of the *in situ* BBB penetration for the data set except for the three LAT substrates (leucine, gabapentin, and phenylalanine), which were underestimated by the *in vitro* PBMEC. The compounds that were highly permeable *in situ*, including diazepam and testerostone, demonstrated a high permeability in the PBMEC model. The compounds with moderate permeability *in situ* (theophylline, quinidine, metoprolol, phenytoin, dopamine, and caffeine) were found to have a moderate permeability in PBMEC. Lastly, a similar trend emerged for the low permeability compounds (sucrose, mannitol, taurocholic acid, methotrexate and vinblastine). Furthermore, Figure 8 depicts the correlation between the $logP_e$ values measured in the PBMEC model and the logPS values observed *in situ*

for the 15 test compounds (except for diazepam). The PBMEC $logP_e$ correlated with the *in situ* logPS with an r^2 of 0.60 for the 15 compounds. When the three system L substrates were excluded from the correlation, the r^2 increased to 0.89.

Discussion

The main objective of the present study was to develop a simple yet robust *in vitro* BBB cell model to predict the net permeability (passive and active transported processes) of NCEs across the BBB *in vivo*.

Our initial characterization of the PBMEC model suggested that it maintained many important BBB properties. First, the extensive staining with Factor VIII signified the homogeneity of the endothelial cells. Second, visualization of the intercellular tight junctions and the moderate to high TEER values (300-550 $\Omega \bullet cm^2$) indicated an acceptable "tightness" of the PBMEC monolayer. Third, the PBMEC expressed the mRNA of several BBB uptake and efflux transporters, including GLUT1, LAT1, MRP1, MRP4, MRP5, Pgp, and BCRP. Moreover, preliminary study of the functional activity of Pgp in the PBMEC showed that the basolateral-to-apical/apical-to-basolateral (B-to-A/A-to-B) permeability ratio of Rhodamine 123, a Pgp substrate, was 1.73. Addition of a Pgp inhibitor, cyclosporin A, reduced the B-to-A/A-to-B ratio of Rhodamine 123 to 1. The B-to-A/A-to-B permeability ratio of sucrose, the paracellular marker, was 1 under both conditions (data not shown). This apparent polarized transport of the Pgp substrates suggested that P-gp was functionally active and was predominantly located on the apical membrane in the PBMEC. Lastly, the PBMEC model took

only 5-6 days to reach confluence as compared with 10-12 days with the BBMEC model, which added to the advantage of the PBMEC as an *in vitro* BBB screening tool.

One of the continuing challenges to develop an *in vitro* BBB permeability model is the lack of standardized study conditions, which makes it difficult to interpret and compare models from lab to lab. Protocols in the literature describing various *in vitro* BBB models varied in many respects including cell origins, cell isolation procedures, cell culture conditions, and permeability study conditions (Audus and Borchardt 1986b; Rubin et al. 1991; Cecchelli et al. 1999; Franke et al. 2000; Jeliazkova-Mecheva and Bobilya 2003). Therefore, the TEER and sucrose permeability values reported for the primary cultures of BBMEC or PBMEC were highly variable among different laboratories (Pardridge et al. 1990; Rubin et al. 1991; Jeliazkova-Mecheva and Bobilya 2003; Torok et al. 2003) and difficult to compare. Thus, initial experiments were conducted in our laboratory to develop the optimal culture and permeability assay conditions for the present PBMEC model.

First, we tested the influence of a stirred vs. unstirred condition on the permeability measurements in the PBMEC model. Physiologically, there is virtually no unstirred water layer (UWL) at the surface of the endothelium of the *in vivo* brain (Pardridge 1991). However, many *in vitro* permeability studies were conducted under unstirred conditions (Pardridge et al. 1990; Rubin et al. 1991; Franke et al. 2000). It has been reported that in Caco-2 cells, the thickness of the UWL can be greater than 1000 μm under unstirred conditions, which is greater than the thickness of the UWL in the *in vivo* intestinal lumen (30–100 μm) (Lennernas 1998). The increased thickness of the UWL *in vitro* conceivably presents an artificial, rate-limiting barrier to passive diffusion across the cell monolayer. In the present PBMEC model, stirring in both donor and receiver chambers (600 rpm) greatly increased the transendothelial flux of the moderate and

high permeability compounds, but had little effect on the low permeability compounds. In turn, the dynamic range (*i.e*. the ratio of P_e of high permeability compounds to the P_e of low permeability compounds) of PBMEC permeability was greatly increased. These data suggest that permeability studies performed under stirred conditions reduce the influence of the UWL, and therefore, better mimic the *in vivo* BBB environment as compared with unstirred conditions.

Second, considering the close apposition of astrocytes to brain capillary endothelial cells *in vivo*, some researchers speculated that factor(s) produced by astrocytes are important for the establishment of a fully functional BBB *in vitro* (Raub et al. 1992). In fact, co-culture with astrocytes or the culture of *in vitro* BBB cells in ACM has been shown to enhance the tight-junction formation and decrease sucrose permeability in several *in vitro* BBB models (Cecchelli et al. 1999; Megard et al. 2002). However, these results varied from one laboratory to another. Torok et al. (2003) reported that ACM led to a 60% increase in TEER of their PBMEC model, but had no effect on the paracellular permeability of sucrose. In addition, it was found there was only a slight (14%) reduction of the sucrose permeability in the presence of ACM in a BBMEC model (Pardridge et al. 1990). In the present study, PBMEC cells cultured with ACM resulted in only a 10–25 % enhancement of TEER values and showed no effect on the permeability of sucrose. Although still lower than the TEER value *in vivo* (>1000 $\Omega \bullet cm^2$) (Butt et al. 1990), the TEER of the PBMEC model (300-550 $\Omega \bullet cm^2$) were higher than that reported for most other solo-cultures of PBMEC ($\leq$ 400 $\Omega \bullet cm^2$) (Fischer et al. 2000; Jeliazkova-Mecheva and Bobilya 2003; Torok et al. 2003) and BBMEC (80-140 $\Omega \bullet cm^2$) (Rubin et al. 1991), as well as for TR-BBB cells (5-20 $\Omega \bullet cm^2$) (unpublished observation in-house). While the paracellular restrictiveness of the PBMEC model may still warrant further improvement to be close to that reported *in vivo* (e.g., *in vitro* permeability of sucrose of 90 $\times 10^{-6}$ $cm \bullet sec^{-1}$ much higher than that

estimated *in vivo* (0.03-0.1 $\times 10^{-6}$ cm•sec^{-1}) (Levin 1980; Rechthand et al. 1987)), a much tighter monolayer may not be critical for the PBMEC to serve as a BBB permeability screen for assessing low, medium, and high brain penetration. Furthermore, the advantages gained under influence of astrocytes may be offset by a loss of culture precision since concentrations of astrocyte-related factors may differ from study to study.

Third, the PBMEC model from the current study remains viable after more than eight months of storage in liquid nitrogen without significant loss of functionality. The average logP_e of the 16 compounds tested in fresh PBMEC correlated well with those measured from cryopreserved cells, indicating both freshly isolated and cryopreserved PBMEC can be used to perform permeability studies of NCEs.

Upon defining the study conditions in the current PBMEC model (non-ACM culture, stirred condition, and using either fresh or cryopreserved cells), the primary goal of present study was to evaluate whether this PBMEC model could predict the *in vivo* BBB permeability of structurally diverse compounds despite the mechanism of BBB penetration. Correlation between *in situ* or *in vivo* permeability and *in vitro* permeability from primary cultured BMEC models has been reported for a variety of compounds, including small molecules (Guillot et al. 1993; Saheki et al. 1994; Cecchelli et al. 1999) and proteins (Pardridge et al. 1990). However, most previous studies tested either a small number of passive diffusion compounds (Saheki et al. 1994; Cecchelli et al. 1999) or a set of structural analogues (Guillot et al. 1993). In the present study, 8 of the compounds in the test set are known to be influenced by active uptake or efflux transport processes. A strong correlation ($r^2 = 0.89$) between the *in vitro* logP_e and the *in situ* logPS was observed with the three LAT substrates excluded. Consistent with this strong correlation, the rank order of PBMEC permeability of these compounds, except for the system L substrates, was

comparable to that of the *in situ* BBB permeability in rats, with sucrose, mannitol, taurocholic acid, methotrexate, and vinblastine at the low end of the permeability range, theophylline, quinidine, phenytoin, metoprolol, dopamine, and caffeine in the moderate permeability range, and testosterone and diazepam at the high end of the permeability range. Moreover, this is the first study to demonstrate a significant quantitative correlation between the *in vitro* and *in situ* permeabilities of compounds that are known substrates of active efflux transporters at the BBB, including Pgp (vinblastine and quinidine), and MRP (taurocholic acid, phenytoin and methotrexate). This data provides clear evidence of the net activity of major BBB transporters in the PBMEC model.

However, the PBMEC underestimated the *in situ* BBB permeability for the three LAT substrates (phenylalanine, leucine, and gabapentin). One of the possible explanations is species difference in LAT expression level between rat and porcine at the BBB. Another explanation for this discrepancy may be down-regulation of LAT expression and/or function *in vitro*, which has been suggested by Pardridge et al. (1990). Preliminary data in our laboratory has demonstrated that the uptake of radiolabeled leucine into the PBMEC monolayers is a saturable process with an apparent K_m of 170 μM, which is close to that reported both *in vivo* and *in vitro* (Cardelli-Cangiano et al. 1981; Audus and Borchardt 1986a). However, RT-PCR analysis shows mRNA expression of both LAT1 and LAT2 in the PBMEC model. *In vivo*, LAT1 protein is highly expressed in the BBB with little, if any, expression of LAT2 (Kageyama et al. 2000). The apparent expression of LAT2 in the current PBMEC model may suggest modulation of LAT expression in the PBMEC *in vitro*. Nevertheless, while amino acid transporter activity would be a beneficial feature of the PBMEC model, it may not be essential for the potential application of the PBMEC model as a screening tool for the majority of non-amino acid CNS compounds.

In summary, our data show that the PBMEC model maintains the complexities of the *in vivo* BBB such as complex tight-junctions, moderate to high electrical resistance, and mRNA expression of active transporters. Most importantly, the current PBMEC model demonstrates the ability to predict the net passive and transporter-mediated BBB penetration with high success, medium throughput, and high reproducibility, thus, allowing the PBMEC model to be used as an effective BBB permeability screening tool in pharmaceutical research.

Acknowledgements

We would like to thank Dr. Xinrong Liu from Groton PDM for assisting in the transfer of the *in situ* brain perfusion assay to our site. We would also like to thank Dr. Susan Buist and Dr. Joe Ware for reviewing and providing helpful comments during the preparation of this manuscript.

References

Audus K. L. and Borchardt R. T. (1986a) Characteristics of the large neutral amino acid transport system of bovine brain microvessel endothelial cell monolayers. *J Neurochem* **47,** 484-488.

Audus K. L. and Borchardt R. T. (1986b) Characterization of an in vitro blood-brain barrier model system for studying drug transport and metabolism. *Pharm. Res.* **3,** 81-87.

Bowman P. D., Ennis S. R., Rarey K. E., Betz A. L. and Goldstein G. W. (1983) Brain microvessel endothelial cells in tissue culture: a model for study of blood-brain barrier permeability. *Ann Neurol* **14,** 396-402.

Butt A. M., Jones H. C. and Abbott N. J. (1990) Electrical resistance across the blood-brain barrier in anaesthetized rats: a developmental study. *J Physiol* **429,** 47-62.

Cardelli-Cangiano P., Cangiano C., James J. H., Jeppsson B., Brenner W. and Fischer J. E. (1981) Uptake of amino acids by brain microvessels isolated from rats after portacaval anastomosis. *J Neurochem* **36,** 627-632.

Casella G. and Berger R. (1990) *Statistical Inference*. Duxbury Press, Belmont, California.

Cecchelli R., Dehouck B., Descamps L., Fenart L., Buee-Scherrer V. V., Duhem C., Lundquist S., Rentfel M., Torpier G. and Dehouck M. P. (1999) In vitro model for evaluating drug transport across the blood-brain barrier. *Adv Drug Deliv Rev* **36,** 165-178.

Drion N., Lemaire M., Lefauconnier J. M. and Scherrmann J. M. (1996) Role of P-glycoprotein in the blood-brain transport of colchicine and vinblastine. *J Neurochem* **67,** 1688-1693.

Fischer S., Wobben M., Kleinstuck J., Renz D. and Schaper W. (2000) Effect of astroglial cells on hypoxia-induced permeability in PBMEC cells. *Am J Physiol Cell Physiol* **279,** C935-944.

Franke H., Galla H. and Beuckmann C. T. (2000) Primary cultures of brain microvessel endothelial cells: a valid and flexible model to study drug transport through the blood-brain barrier in vitro. *Brain Res Brain Res Protoc* **5,** 248-256.

Guillot F., Misslin P. and Lemaire M. (1993) Comparison of fluvastatin and lovastatin blood-brain barrier transfer using in vitro and in vivo methods. *J Cardiovasc Pharmacol* **21,** 339-346.

Hargreaves K. M. and Pardridge W. M. (1988) Neutral amino acid transport at the human blood-brain barrier. *J Biol Chem* **263,** 19392-19397.

Jeliazkova-Mecheva V. V. and Bobilya D. J. (2003) A porcine astrocyte/endothelial cell co-culture model of the blood-brain barrier. *Brain Res Brain Res Protoc* **12,** 91-98.

Kageyama T., Nakamura M., Matsuo A., Yamasaki Y., Takakura Y., Hashida M., Kanai Y., Naito M., Tsuruo T., Minato N. and Shimohama S. (2000) The 4F2hc/LAT1 complex transports L-DOPA across the blood-brain barrier. *Brain Res* **879,** 115-121.

Kitazawa T., Terasaki T., Suzuki H., Kakee A. and Sugiyama Y. (1998) Efflux of taurocholic acid across the blood-brain barrier: interaction with cyclic peptides. *J Pharmacol Exp Ther* **286,** 890-895.

Kusuhara H, Suzuki H, Terasaki T, Kakee A, Lemaire M and Sugiyama Y (1997) P-glycoprotein mediates the efflux of quinidine across the blood-brain barrier. *J. Pharmacol. Exp. Ther.* **283:**574-580.

Lennernas H. (1998) Human intestinal permeability. *J Pharm Sci* **87,** 403-410.

Levin V. A. (1980) Relationship of octanol/water partition coefficient and molecular weight to rat brain capillary permeability. *J Med Chem* **23,** 682-684.

Lin L. I. (2000) Total deviation index for measuring individual agreement with applications in laboratory performance and bioequivalence. *Stat Med* **19,** 255-270.

Liu X., Tu M., Kelly R. S., Chen C. and Smith B. J. (2004) Development of a computational approach to predict blood-brain barrier permeability. *Drug Metab Dispos* **32,** 132-139.

Mark K. S. and Miller D. W. (1999) Increased permeability of primary cultured brain microvessel endothelial cell monolayers following TNF-alpha exposure. *Life Sci* **64,** 1941-1953.

Martel C. L., Mackic J. B., Adams J. D., Jr., McComb J. G., Weiss M. H. and Zlokovic B. V. (1996) Transport of dopamine at the blood-brain barrier of the guinea pig: inhibition by psychotropic drugs and nicotine. *Pharm Res* **13,** 290-295.

McCall A. L., Millington W. R. and Wurtman R. J. (1982) Blood-brain barrier transport of caffeine: dose-related restriction of adenine transport. *Life Sci* **31,** 2709-2715.

McCarthy K. D. and de Vellis J. (1980) Preparation of separate astroglial and oligodendroglial cell cultures from rat cerebral tissue. *J Cell Biol* **85,** 890-902.

Megard I., Garrigues A., Orlowski S., Jorajuria S., Clayette P., Ezan E. and Mabondzo A. (2002) A co-culture-based model of human blood-brain barrier: application to active transport of indinavir and in vivo-in vitro correlation. *Brain Res* **927,** 153-167.

Miller D. S., Nobmann S. N., Gutmann H., Toeroek M., Drewe J. and Fricker G. (2000) Xenobiotic transport across isolated brain microvessels studied by confocal microscopy. *Mol Pharmacol* **58,** 1357-1367.

Miller D. W., Audus K. L. and Borchardt R. T. (1992) Application of cultured bovine brain endothelial cells in the study of the blood-brain barrier. *J. Tissue Culture Methods* **14,** 217-224.

Murakami H., Takanaga H., Matsuo H., Ohtani H. and Sawada Y. (2000) Comparison of blood-brain barrier permeability in mice and rats using in situ brain perfusion technique. *Am J Physiol Heart Circ Physiol* **279,** H1022-1028.

Oldendorf W. H. (1971) Brain uptake of radiolabeled amino acids, amines, and hexoses after arterial injection. *Am J Physiol* **221,** 1629-1639.

Pardridge W. M. (1983) Brain metabolism: a perspective from the blood-brain barrier. *Physiol Rev* **63,** 1481-1535.

Pardridge W. M. (1991) *Peptide drug delivery to the brain*. Raven Press, New York.

Pardridge W. M., Triguero D., Yang J. and Cancilla P. A. (1990) Comparison of in vitro and in vivo models of drug transcytosis through the blood-brain barrier. *J Pharmacol Exp Ther* **253,** 884-891.

Potschka H. and Loscher W. (2001) Multidrug resistance-associated protein is involved in the regulation of extracellular levels of phenytoin in the brain. *Neuroreport* **12,** 2387-2389.

Raub T. J., Kuentzel S. L. and Sawada G. A. (1992) Permeability of bovine brain microvessel endothelial cells in vitro: barrier tightening by a factor released from astroglioma cells. *Exp Cell Res* **199,** 330-340.

Rechthand E., Smith Q. R. and Rapoport S. I. (1987) Transfer of nonelectrolytes from blood into peripheral nerve endoneurium. *Am J Physiol* **252,** H1175-1182.

Reichel A., Abbott N. J. and Begley D. J. (2002) Evaluation of the RBE4 cell line to explore carrier-mediated drug delivery to the CNS via the L-system amino acid transporter at the blood-brain barrier. *J Drug Target* **10,** 277-283.

Root C., Smith C. D., Winegar D. A., Brieaddy L. E. and Lewis M. C. (1995) Inhibition of ileal sodium-dependent bile acid transport by 2164U90. *J Lipid Res* **36,** 1106-1115.

Rubin L. L., Hall D. E., Porter S., Barbu K., Cannon C., Horner H. C., Janatpour M., Liaw C. W., Manning K., Morales J. and et al. (1991) A cell culture model of the blood-brain barrier. *J Cell Biol* **115,** 1725-1735.

Saheki A., Terasaki T., Tamai I. and Tsuji A. (1994) In vivo and in vitro blood-brain barrier transport of 3-hydroxy-3-methylglutaryl coenzyme A (HMG-CoA) reductase inhibitors. *Pharm Res* **11,** 305-311.

Schinkel A. H., Wagenaar E., Mol C. A. and van Deemter L. (1996) P-glycoprotein in the blood-brain barrier of mice influences the brain penetration and pharmacological activity of many drugs. *J Clin Invest* **97,** 2517-2524.

Smith Q. R. (1991) The blood-brain barrier and the regulation of amino acid uptake and availability to brain. *Adv Exp Med Biol* **291,** 55-71.

Smith Q. R. (1996) Brain perfusion systems for studies of drug uptake and metabolism in the central nervous system. *Pharm Biotechnol* **8,** 285-307.

Su TZ, Lunney E, Campbell G and Oxender DL (1995) Transport of gabapentin, a gamma-amino acid drug, by system l alpha-amino acid transporters: a comparative study in astrocytes, synaptosomes, and CHO cells. *J Neurochem.* **64:**2125-2131.

Terasaki T. and Hosoya K. (2001) Conditionally immortalized cell lines as a new in vitro model for the study of barrier functions. *Biol Pharm Bull* **24,** 111-118.

Torok M., Huwyler J., Gutmann H., Fricker G. and Drewe J. (2003) Modulation of transendothelial permeability and expression of ATP-binding cassette transporters in cultured brain capillary endothelial cells by astrocytic factors and cell-culture conditions. *Exp Brain Res* **153,** 356-365.

Zhang Y., Han H., Elmquist W. F. and Miller D. W. (2000) Expression of various multidrug resistance-associated protein (MRP) homologues in brain microvessel endothelial cells. *Brain Res* **876,** 148-153.

Current address:

[1]Dr. Yan Zhang

Drug Metabolism and Biopharmaceutics

Incyte Corporation

Henry Clay Road and Rt 141

Wilmington, DE 19880

[1]Dr. Madhu Cherukury

Drug Metabolism and Pharmacokinetics

Abbott Bioresearch Center

100 Research Drive

Worcester, MA 01605

Legends for Figures

Fig. 1
Phase contrast microscopy of primary cultured PBMEC on culture day 2 (a), day 4 (b), and day 6 (c) (100 X magnification).

Fig. 2
Immunostaining of PBMEC monolayers with anti-von Willebrand Factor VIII poly-clonal antibody (green fluorescence) (a). The negative controls were incubated with normal rabbit IgG (b). Cell nuclei are counterstained with DAPI (blue fluorescence).

Fig. 3
Transmission electron microscopy of PBMEC grown on collagen-coated, fibronectin-treated chamber slides. Two adjacent cells with slightly overlapping membrane (a, 2100 X magnification; b, 11,000 X magnification). Two adjacent cells with direct contact (c, 3800 X magnification; d, 15,000 X magnification). Arrows indicate the tight junction formation.

Fig. 4

RT-PCR analysis of transporter mRNA and tight junction protein mRNA expression in total RNA samples prepared from confluent PBMEC. 100bp DNA ladders are shown in lanes 1 and 13. Lane 2, ZO-1; Lane 3, GLUT1; Lane 4, LAT1; Lane 5, LAT2; Lane 6, MRP1; Lane 7, MRP2; Lane 8, MRP4; Lane 9, MRP5; Lane 10, MDR1; Lane 11, BCRP; Lane 12, GAPDH.

Fig. 5

TEER values of PBMEC monolayers on various days in cultures. Each data point represents the mean ± SD of 6 cell monolayers each day and results are from 13 isolations. The bar indicates TEER at 300 $\Omega \bullet cm^2$, under which no permeability studies were performed.

Fig. 6

Comparison of the TEER values between PBMEC treated with or without ACM. Each data point represents the mean ± SD of 6 cell monolayers each day in culture. *$p<0.05$, Student's t-test.

Fig. 7

Comparison of average $logP_e$ in freshly isolated PBMEC with cyropreserved PBMEC by Total Deviation Index approach (TDI). Studies were performed under stirred conditions. Each data point represents the mean of at least 3 cell monolayers per experimental group. TDI80% refers to the boundary such that at least 80% of the measurements are within 0.1 $logP_e$ units of each other. TDI95% refers to the boundary such that at least 95% of the measurements are within 0.16 log P_e units of each other.

Fig. 8

Correlation between *in vitro* $logP_e$ from PBMEC and logPS determined by *in situ* brain perfusion in rats. The $logP_e$ value represents the mean ± SE of at least 6 cell monolayers for each test compound. The full test set correlated with an r^2 of 0.60. The r^2 increased to 0.89 when the three system L substrates were excluded from the correlation (shown with the dotted line in the figure).

Table 1 Chemical class, BBB transport mechanism, and *in situ* logPS values of the 16 compounds selected for method development in the PBMEC model

Compounds	Chemical class	BBB transport mechanisms	logPS (ml/sec/g)
Sucrose	Neutral	Passive Diffusion	-4.80 [k]
Mannitol	Neutral	Passive Diffusion	-4.30 [k]
Taurocholic acid	Acid	Active Uptake/Efflux [a]	-4.10 [j]
Methotrexate	Acid	Passive Diffusion/Active Efflux (MRP) [b]	-3.88 [j]
Vinblastine	Neutral	Passive Diffusion/Active Efflux (P-gp) [c]	-3.50 [j]
Quinidine	Base	Passive Diffusion/Active Efflux (P-gp) [d]	-2.90 [j]
Theophylline	Neutral	Passive Diffusion	-2.70 [j]
Metoprolol	Neutral	Passive Diffusion	-2.52 [l]
Gabapentin	Amino Acid	Active Uptake (system L) [e]	-2.48 [l]
Phenytoin	Neutral	Passive Diffusion/Active Efflux (MRP) [f]	-2.20 [j]
Dopamine	Base	Passive Diffusion/Active Uptake [g]	-2.10 [j]
Caffeine	Neutral	Passive Diffusion/Active Uptake [h]	-2.00 [j]
Leucine	Amino Acid	Active Uptake (system L) [i]	-1.79 [l]
Phenylalanine	Amino Acid	Active Uptake (system L) [i]	-1.30 [j]
Diazepam	Base	Passive Diffusion	NC*

Testosterone	Neutral	Passive Diffusion	-1.10 [j]

*NC, not calculable
[a] (Kitazawa et al., 1998)
[b] (Miller et al., 2000)
[c] (Drion et al., 1996)
[d] (Kusuhara et al., 1997)
[e] (Su et al., 1995)
[f] (Potschka and Loscher, 2001)
[g] (Martel et al., 1996)
[h] (McCall et al., 1982)
[i] (Hargreaves and Pardridge, 1988)
[j] Liu et al. (Liu et al. 2004)
[k] Murakami et al. (Murakami et al. 2000)
[l] reported from our laboratory using the same method as Liu et al. (2004) and Murakami et al. (2000)

Table 2 Primers used in RT-PCR studies.

Target Gene	Forward Primer	Reverse Primer	Accession Number	Species	Size of PCR product*
MDR1	ACAACATTTACAATCC AGTCTAATAAGAA	ATAAAAGAAATAATTCC AAGGATTAGAAA	AF403245	Pig	338
MRP1	AGTGTGTGGGCAACT GCATCGTCCTGTTT	ATCGATGGTGACATTGA TGTGCTTGAGAAC	AF403246	Pig	354
MRP2	ATGTGTCTTTTCCTGG ATTATCTCCAACA	TCTGGCGGAGGCCTCTT ATACAGTACA	AF403247	Pig	295
MRP4	CCATTGAAGATCTTCC TGG	GGTGTTCAATCTGTGTGC	NM-005845	Human, rat, mouse	239
MRP5	GGATAACTTCTCAGTG GG	GGAATGGCAATGCTCTA AAG	NM-005688	Human, rat, mouse	381
BCRP	AGTTTATCCGTGGTGT GTCTGGAGGAGAA	TTCAGGAGCAAAAGGAC AGCATTTGCTGTG	AJ420927	Pig	144
GLUT1	AGATGCTGATCCTGG GCCGCTTCATCAT	CTGGACGTCCTCTACTTC CTTCTCTCA	AB208987	Human, rat, mouse	384
LAT1	ACTTGAATTTCGTCAC AGAGGAAATGAT	AGTTGATGACGGAGAAG ATGTCCTTGGAGA	AB018009	Human, rat, mouse	421
LAT2	TGTTTGTAAACGCGAG TGACCAGAAAGTGT	ATGATGTTCCCTACGATG ATACAGGCA	AB037669	Human, rat, mouse	360

ZO-1	ACAGCTACAGGAAAA TGACCGAGTTGCAAT	CCATCTCTTGCTGCCAAA CTATCTTGTGAA	BC036090	Human, rat, mouse	420
GAPDH	ATGGTGAAGGTCGGA GTGAACGGATT	AAGCAGTTGGTGGTACA GGAGGCATT	AF017079	Pig	463

* Estimated based on corresponding porcine or human gene sequence.

Table 3 Comparison of P_e values in PBMEC under stirred and unstirred conditions.

Compound	P_e (x 10^{-6} cm/sec) [a]		Ratio of P_e (test compound / sucrose)		Permeability
	Stirred	Unstirred	Stirred	Unstirred	
Sucrose	92	54	1.0	1.0	Low
Mannitol	108	87	1.2	1.6	
Taurocholic acid	84	68	0.9	1.3	
Vinblastine	140	95	1.5	1.8	
Phenylalanine	248	122	2.7	2.3	Medium
Caffeine	1354	226	15	4.2	
Testostorone	3702	915	40	17	High
Diazepam	5800	1872	63	35	

[a] Data represents the means of at least 3 cell monolayers per experimental group.

Table 4 Summary of the *in vitro* permeability of the sixteen compounds tested in PBMEC

Compounds	P_{app} [a] ($x10^{-6}$ cm/sec)	P_m [a] ($x10^{-6}$ cm/sec)	P_e [a] ($x10^{-6}$ cm/sec)	log P_e (cm/sec)
Sucrose	80 ± 6	682 ± 10	92 ± 24	-4.07
Mannitol	94 ± 6	765 ± 14	107 ± 19	-3.99
Taurocholic acid	72 ± 5	521 ± 7	84 ± 20	-4.09
Methotrexate	107 ± 7	669 ± 12	127 ± 40	-3.90
Vinblastine	107 ± 6	530 ± 9	140 ± 41	-3.88
Theophylline	185 ± 6	824 ± 7	241 ± 27	-3.62
Quinidine	272 ± 7	764 ± 12	422 ± 85	-3.38
Metoprolol	274 ± 8	640 ± 6	486 ± 98	-3.32
Gabapentin	107 ± 6	805 ± 8	124 ± 33	-3.91
Phenytoin	240 ± 7	841 ± 7	336 ± 60	-3.47
Dopamine	590 ± 11	1329 ± 18	1066 ± 173	-2.97
caffeine	416 ± 4	600 ± 7	1354 ± 192	-2.87
Leucine	224 ± 7	890 ± 8	299 ± 50	-3.52
Phenylalanine	192 ± 8	849 ± 12	248 ± 66	-3.61
Diazepam	746 ± 7	857 ± 9	5800 ± 3134	-2.24
Testostorone	639 ± 8	786 ± 9	3702 ± 1458	-2.45

[a] Values represent the means ± SE of data from at least two experiments in triplicates

Fig. 1

a

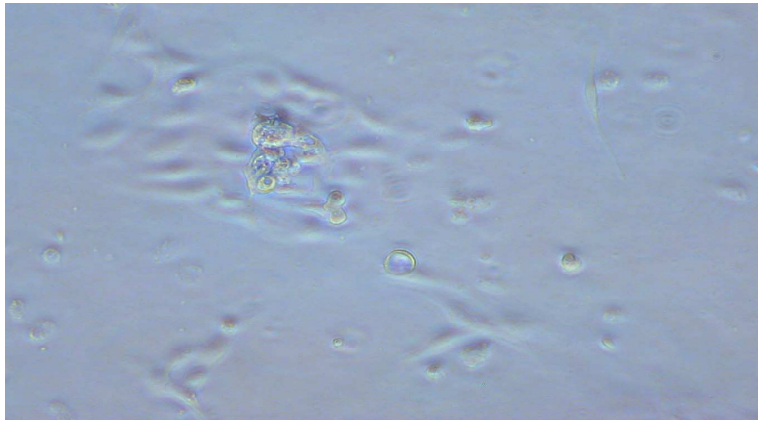

b

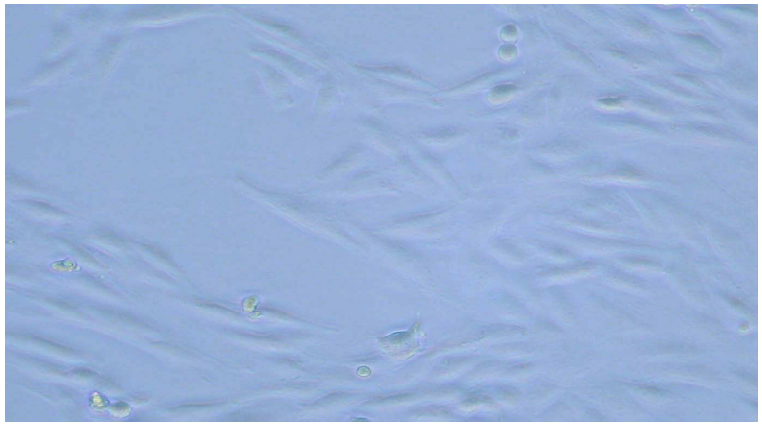

c

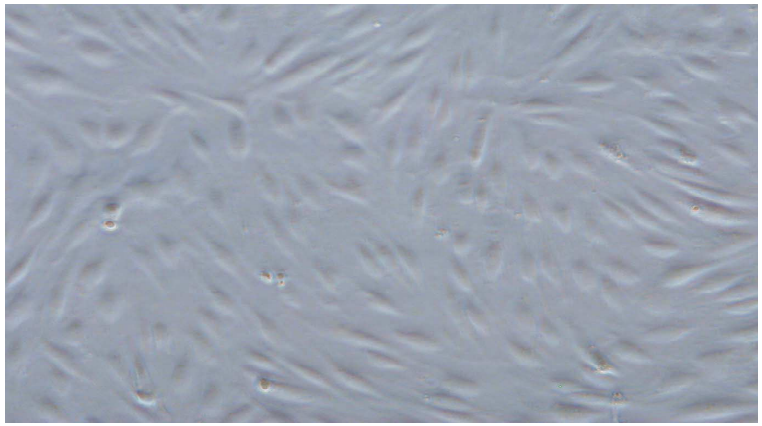

Fig. 2

a

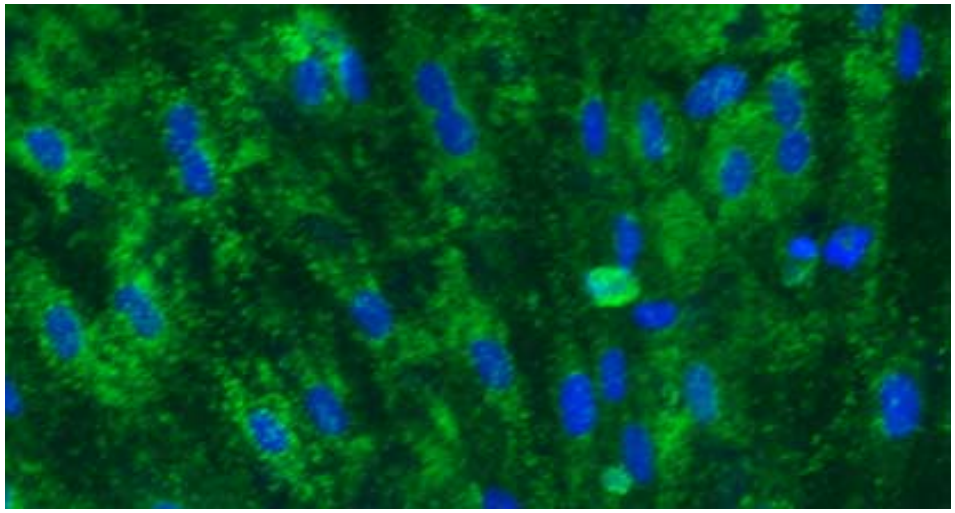

b

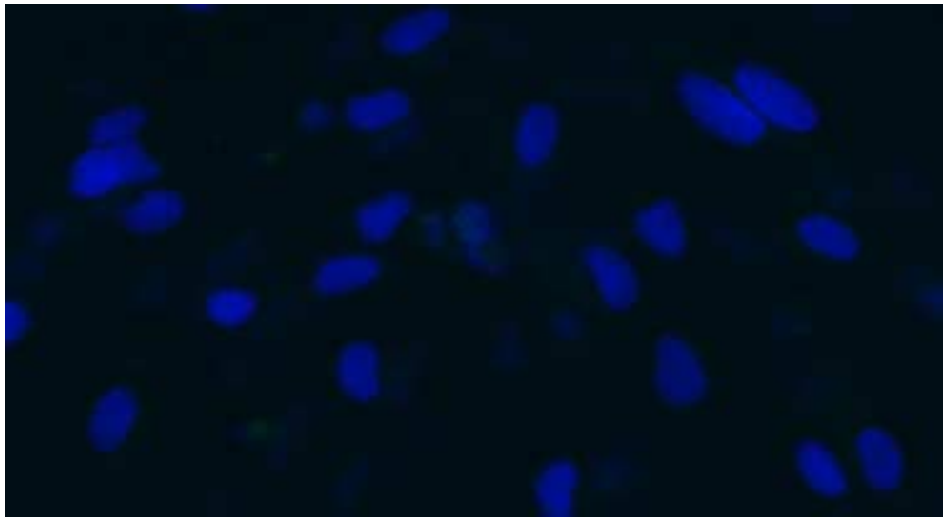

Figure 3

a

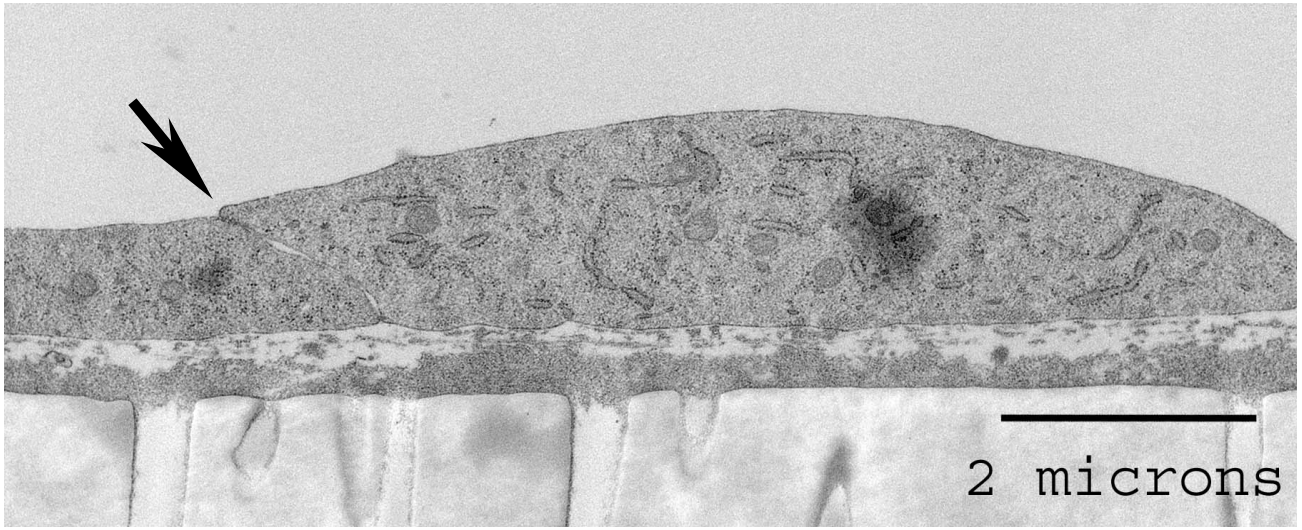

b

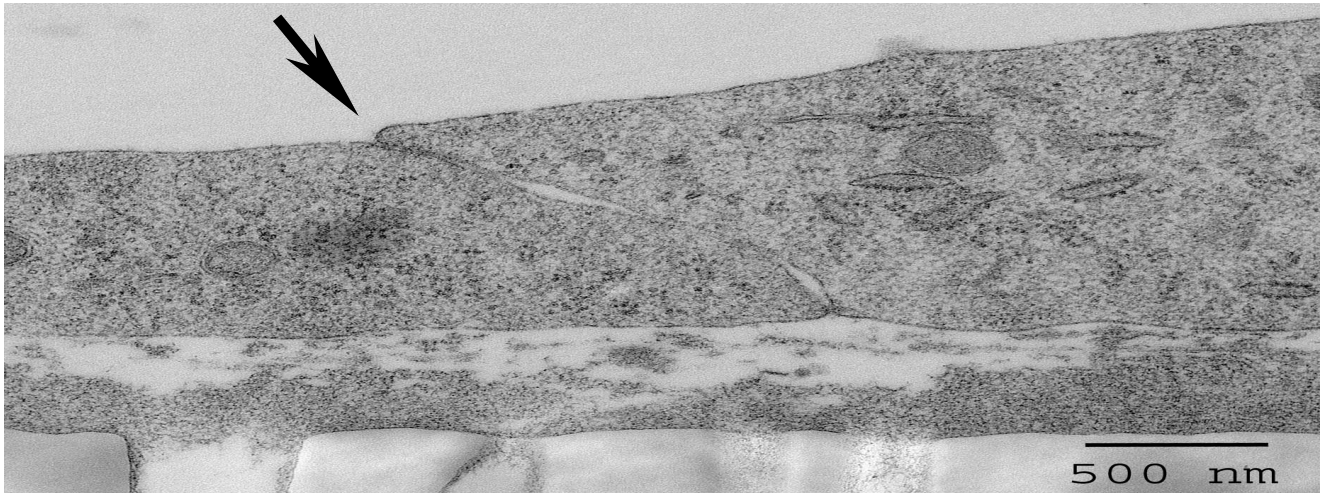

Figure 3

c

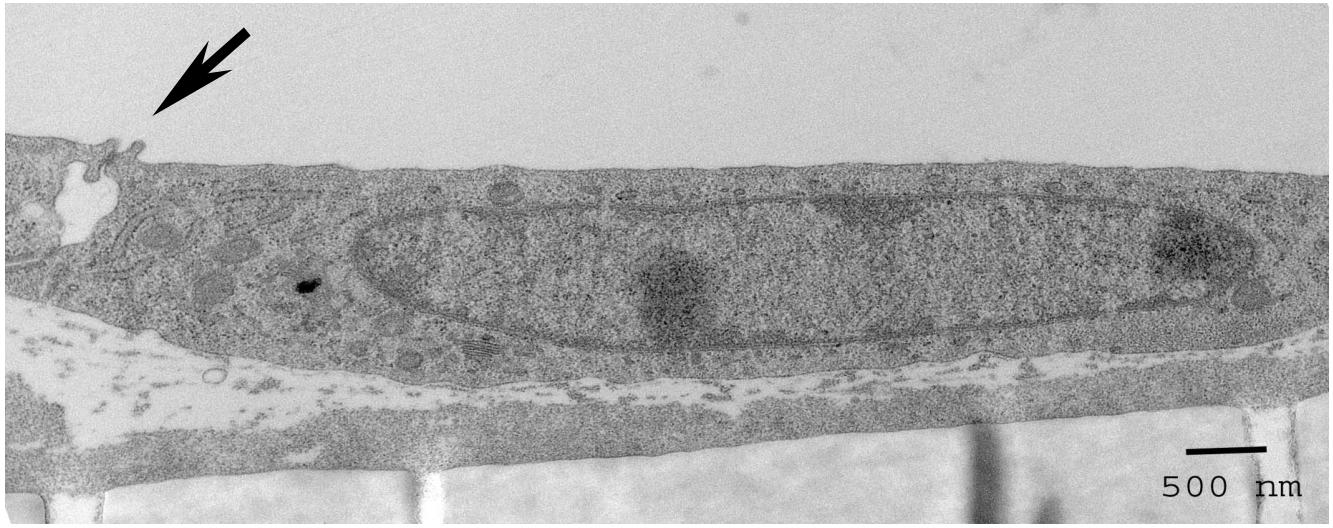

d

Figure 4.

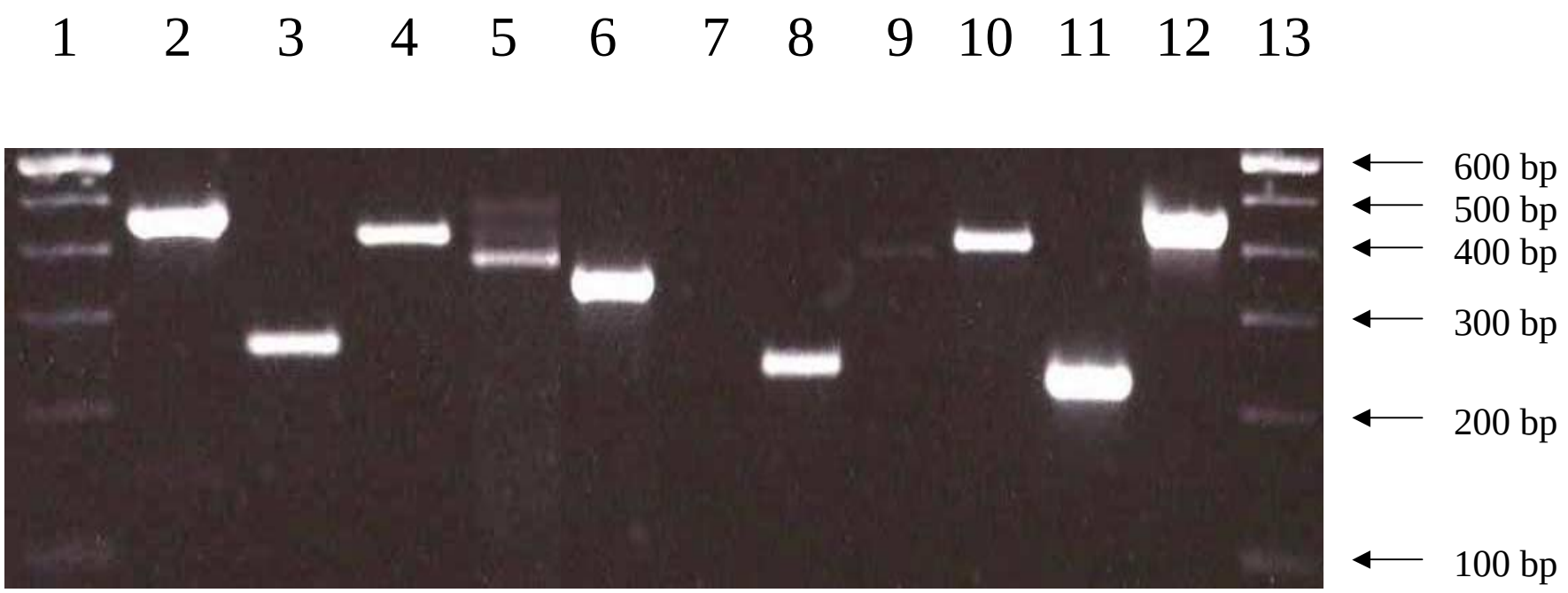

Figure 5.

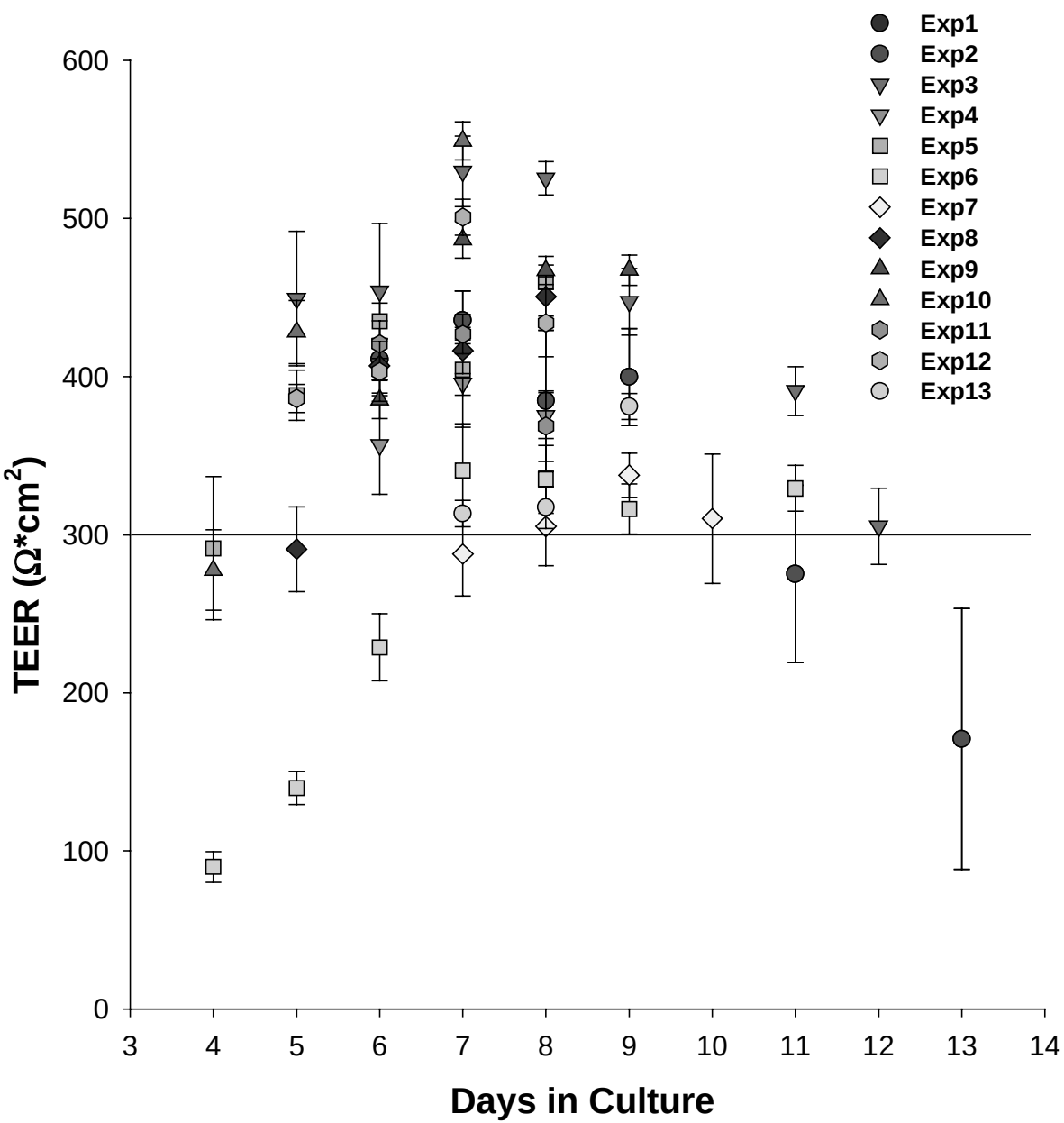
Exp1
Exp2
Exp3
Exp4
Exp5
Exp6
Exp7
Exp8
Exp9
Exp10
Exp11
Exp12
Exp13
TEER (Ω*cm²)
0
100
200
300
400
500
600
3
4
5
6
7
8
9
10
11
12
13
14
Days in Culture

Figure 6.

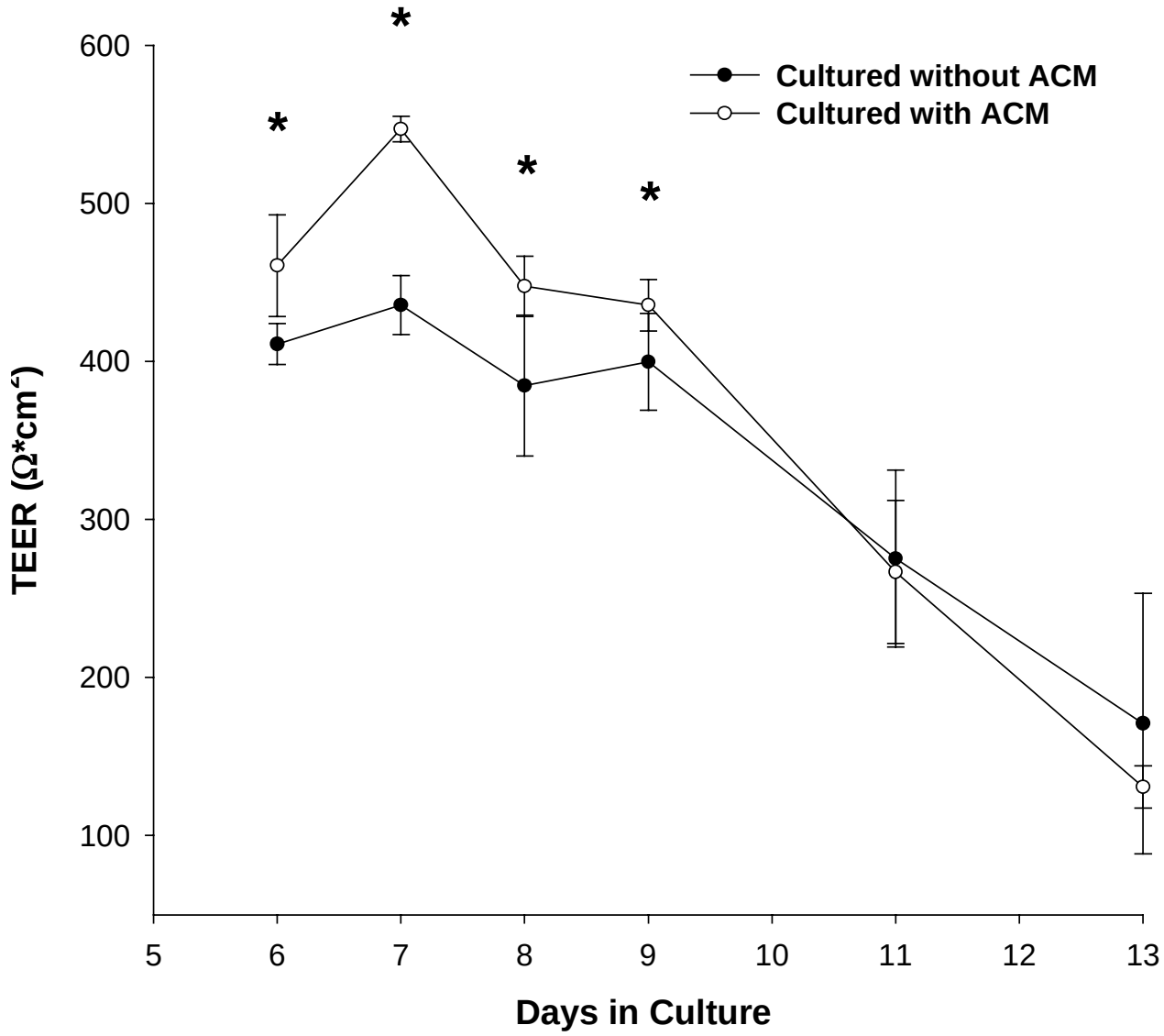

*P<0.05, Student's t-test

Figure 7.

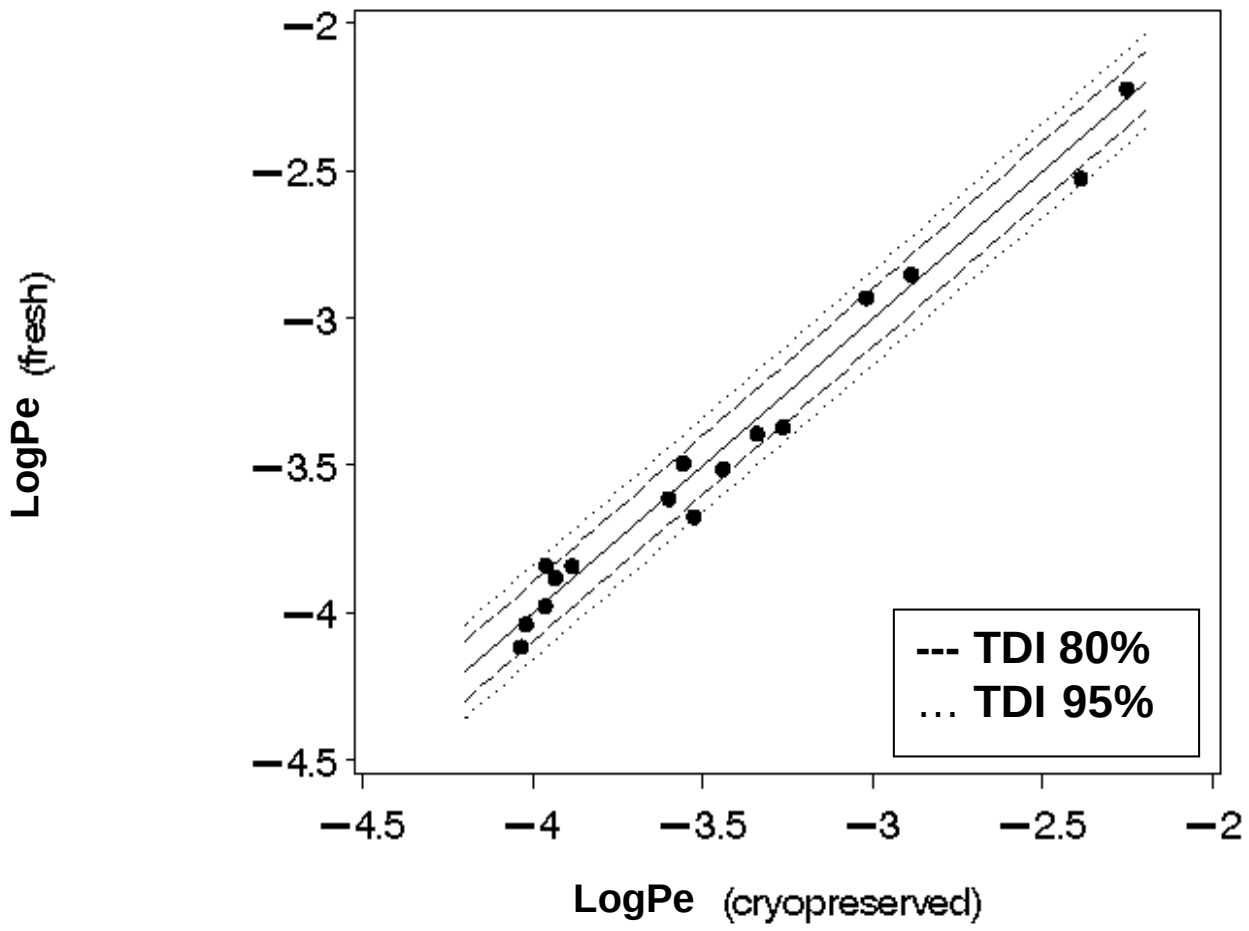
LogPe (fresh)
−2
−2.5
−3
−3.5
−4
−4.5
−4.5
−4
−3.5
−3
−2.5
−2
LogPe (cryopreserved)
--- TDI 80%
… TDI 95%

Figure 8.

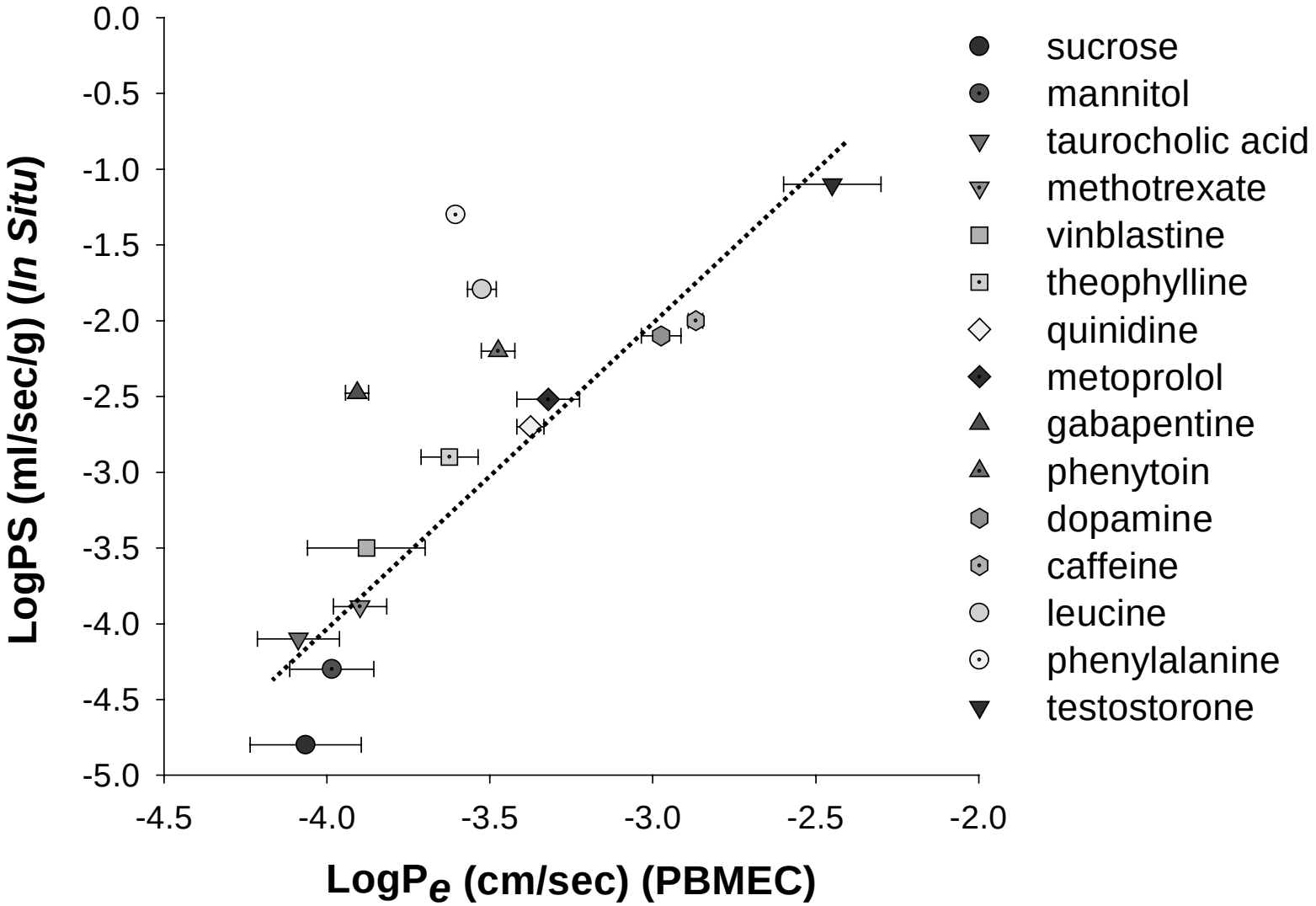
0.0
-0.5
-1.0
-1.5
-2.0
-2.5
-3.0
-3.5
-4.0
-4.5
-5.0
-4.5
-4.0
-3.5
-3.0
-2.5
-2.0
LogPS (ml/sec/g) (In Situ)
LogPe (cm/sec) (PBMEC)
sucrose
mannitol
taurocholic acid
methotrexate
vinblastine
theophylline
quinidine
metoprolol
gabapentine
phenytoin
dopamine
caffeine
leucine
phenylalanine
testostorone